Shear-Induced Collapse in a Lyotropic Lamellar Phase

L. Porcar,[1,2] G. G. Warr,[3] W. A. Hamilton,[4] and P. D. Butler[1]

[1] *National Institute of Standards and Technology, Center for Neutron Research, Gaithersburg, Maryland 20899, USA*
[2] *University of Maryland, College Park, Maryland 20742, USA*
[3] *School of Chemistry, The University of Sydney, Sydney, New South Wales 2006, Australia*
[4] *Condensed Matter Sciences Division, Oak Ridge National Laboratory, Oak Ridge, Tennessee 37831, USA*

(Received 15 December 2004; revised manuscript received 3 May 2005; published 11 August 2005)

An entropically stabilized cetylpyridinium chloride, hexanol, and heavy brine lyotropic lamellar phase subjected to shear flow has been observed here by small angle neutron scattering to undergo collapse of smectic order above a threshold shear rate. The results are compared with theories predicting that such a lamellar phase sheared above a critical rate should lose its stability by a loss of resistance to compression due to the suppression of membrane fluctuations.

DOI: 10.1103/PhysRevLett.95.078302 PACS numbers: 83.10.Tv, 61.12.Ex, 82.70.Uv

Bilayer membranes are the most abundant geometry of self-assembled amphiphiles in nature. They have attracted much attention in both basic and applied science because of their applications in biology, cosmetics, and medicine [1]. Membrane phases commonly display smectic order by stacking flexible fluid bilayers with a periodicity d as in the birefringent anisotropic L_α lamellar phase [2]. They also may form a meandering interface separating two interpenetrating labyrinths of solvent (a sponge L_3 phase [3,4]), or they can consist of locally closed unilamellar or multilamellar vesicles, dispersed in solvent [5].

Many recent studies of membrane phases have focused on characterizing their structural response to shear flow, as hydrodynamic forces can couple to specific fluctuations and induce instabilities leading to structural transformations. An example of such a shear-induced structural change has been described previously [6,7], where we showed that adding an inert thickener to the cetylpyridinium (CPCl) hexanol mixed membrane system [8] significantly slows membrane dynamics, making it possible to transform a sponge into a stacked, passage free, lamellar phase (L_α) by application of steady shear. This transition scales with membrane volume fraction, ϕ, and solvent viscosity, η, according to $\dot{\gamma}\eta/\phi^3$, where $\dot{\gamma}$ is the applied shear rate, in excellent agreement with theoretical predictions [6,7,9]. On cessation of shear, the L_α state relaxes into its equilibrium sponge phase by rapidly reestablishing all of the passages between membranes [10].

Extensive nonequilibrium "phase diagrams" have shown that L_α phases typically exhibit two stationary states under shear [11–14]. The perpendicular "a" orientation corresponds to a membrane with the normals aligned parallel to the vorticity direction (Z), and the parallel "c" orientation, where they align along the velocity gradient direction (∇V) [15]. Hydrodynamic instabilities can also induce more complicated structures. Pioneering studies by Roux *et al.* [16,17] found three distinct steady-state membrane structures, separated by out-of-equilibrium transitions: at low shear rates, the membranes are strongly aligned in the c orientation. At intermediate shear rates, a dynamic transition occurs into multilamellar vesicles of well-defined and shear-rate-dependent size, called "onions" or spherulites [18–21]. At even higher shear rates, the lamellae reorient into the c alignment, but with no defects or dislocations in the flow direction. While the mechanism and kinetics of multilamellar vesicle formation is still unclear [22–24], their formation has been shown to depend on the type and density of defects present in the quiescent lamellae, but not on the nature of the stabilizing interaction [25,26].

In this work we examine the shear-response of a lamellar phase with a near-zero density of focal conic domains of the second kind. Bruinsma and Rabin predicted that a c-aligned, defect-free lyotropic lamellar phase stabilized by entropic or fluctuation interactions should undergo a strong instability above a threshold shear rate given by $\dot{\gamma}_c \cong (k_B T)^{5/2}/(\eta\kappa^{3/2}d^3)$ [27]. Here k_B, T, η, κ, and d are the Boltzmann constant, temperature, viscosity, membrane bending rigidity, and intermembrane separation, respectively. Above this shear rate, such a lamellar phase should lose its stability via a loss of resistance to compression as shear suppresses the amplitude of out-of-plane membrane fluctuations, negating the entropic repulsion. Similar scaling was predicted by Ramaswamy for a aligned membranes [28].

Al kahwaji and Kellay [29] recently reported a turbidity onset and increased small angle light scattering in freely suspended thin films with membranes in an assumed a orientation under shear as a signature of lamellar collapse, tending to support these predictions. By analyzing the position and shape of the lamellar Bragg peak in light scattering, Yamamoto and Tanaka [30] similarly argued that shear elastically deforms membranes and suppresses fluctuations in hyperswollen lamellar phases.

Here we demonstrate experimentally how shear induces collapse in an undulating lamellar phase with few defects. The system studied here is similar to that used previously [6,7,10] and consists of cetylpyridinium chloride plus hexanol membranes in brine (0.2 M sodium chloride in D_2O) also containing dissolved dextrose. As seen previously, we find the effect of added dextrose on the phase diagram of the CPCl-hexanol-brine system is comparable to that of replacing H_2O with D_2O [7,31]. All samples lay in the hexanol-rich region of the lamellar phase stability domain, determined by the mixing ratio of the membrane-forming components $h = m_{\mathrm{hex}}/m_{\mathrm{CPCl}}$, close to the boundary with the L_3/L_a coexistence region.

Steady-shear small-angle neutron-scattering (SANS) experiments were performed on the NG7 spectrometer at the National Institute of Standards and Technology, Center for Neutron Research. The sample-to-detector distance was 15.5 m and the neutron wavelength 0.6 nm, giving a Q range between 0.04 and 0.2 nm^{-1}. The Couette cell used has a specially designed vapor barrier to minimize evaporation [32]. Two scattering configurations are used (see Fig. 1): in the radial geometry, the neutron beam passes through the sample along the velocity gradient direction, ∇V, and across the diameter of the cylinder, while in the tangential geometry, the beam passes along the flow direction, V, at a tangent to the sample annulus. These configurations allow us to measure the structure in the flow-vorticity (V, Z) and the velocity gradient-vorticity $(\nabla V, Z)$ planes. Raw data are corrected and converted to an absolute scale as described previously [32].

Figure 1 shows the corrected two-dimensional SANS scattering patterns in both radial (V, Z) and tangential $(\nabla V, Z)$ geometries for a membrane volume fraction $\phi = 0.05$ over a wide range of shear rates. After loading, the lamellar phase instantly aligns in the c orientation as Bragg peaks are evident at $Q \sim 0.092\ \mathrm{nm}^{-1}$, characteristic of a smectic order of periodicity approximately 68 nm in the ∇V direction [33]. The radial scattering is rather weak and featureless. At low shear rates, no significant changes are detected in either geometry, but as the shear rate is increased above 600 s^{-1}, an isotropic scattering at very low angle becomes evident in the tangential pattern. At shear rates above 1500 s^{-1}, this signal overwhelms the Bragg peak resulting in a strong, isotropic signal characteristic of large-scale structures. A corresponding scattering at low Q in the Z direction is evident in the radial geometry measurements over the entire range of shear rates.

This clearly shows that shear disrupts the smectic order in this lamellar phase. To quantify the structural response of this system to shear, we averaged the intensities over sectors $\pm 15°$ from the Z and ∇V directions in the radial and tangential patterns, respectively. Because of the low angles used, we have not corrected for beam refraction and dissymmetric sample absorption in the annulus. Figure 2 shows the excess tangential scattering, $I_{\nabla V} - I_Z$, from which the strong, isotropic small angle scattering has been subtracted (using the average of the right part of the 2D pattern). The shape of the Bragg peak changes little at low shear rates ($\dot{\gamma} \leq 600\ \mathrm{s}^{-1}$), although the peak intensity increases slightly as shear improves alignment. With increasing shear rates, the peak becomes broader and less intense, indicating a decrease in the smectic compression modulus [34] and, hence, in intermembrane repulsion. Because the only stabilizing interaction in this system is the Helfrich repulsion and the membrane bending modulus is unaffected by shear, this implies a reduction in the membrane fluctuations. This effect was also observed by Yamamoto *et al.* but for shear rates an order of magnitude lower than that predicted by theory [27,28]. However, no discernible Bragg peak shift is detected within our SANS resolution.

As the shear rate is further increased, the correlation peak disappears and the scattered intensity at high Q decreases, indicating collapse of the entropically stabilized lamellar phase. This change is quite abrupt, occurring over only a 20%–30% change in shear rate, and is reversible. When shear is stopped, the c-aligned lamellar phase is recovered, but the relaxation time is sensitive to sample history. At no shear rates did we see any indication of a shear-induced macroscopic phase separation, shear banding, or turbidity as observed by Al kahwaji *et al.* [29].

According to the model of Bruinsma and Rabin, the shear rate should scale with membrane spacing and solvent viscosity so that $\dot{\gamma}_c \eta d^3 \cong (k_B T)^{5/2}/\kappa^{3/2}$ is constant [27]. Here we have varied the membrane concentration from $\phi = 0.03$ to 0.07, giving lamellar spacings between 50 and 130 nm, at fixed solvent viscosity. The structural response to shear flow may be quantified by the anisotropy

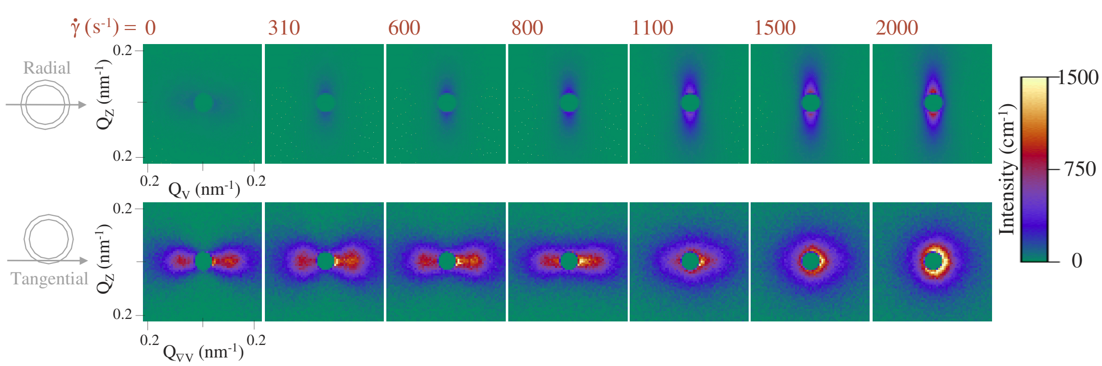

FIG. 1 (color online). Small angle neutron scattering patterns in radial and tangential geometries for a $\phi = 0.05$ lamellar phase as a function of steady shear rate.

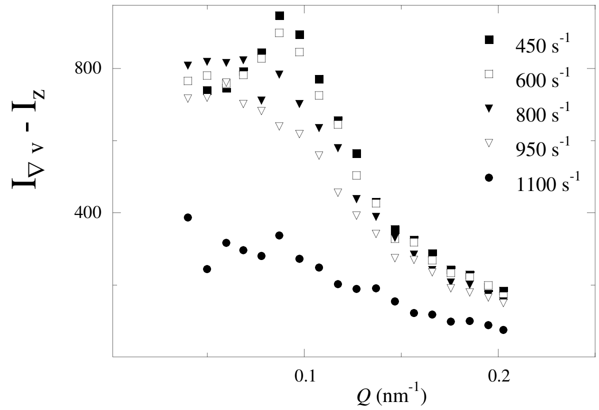

FIG. 2. Excess scattering from the $\phi = 0.05$ lamellar phase in the ∇V direction, $I_{\nabla V} - I_Z$, at various shear rates.

of the tangential scattering pattern, $A_{\mathrm{TAN}} = (I_{\nabla V} - I_Z)/(I_{\nabla V} + I_Z)$. As Fig. 3 shows, A_{TAN} is near 1 at low shear rates for all membrane volume fractions, as expected for strongly aligned lamellae. As the shear rate increases to a critical value, the anisotropy abruptly decreases, indicating collapse. The critical shear rate increases with membrane volume fraction by almost 2 orders of magnitude over the range studied as neighbor membranes confine the amplitude of undulations.

We define the critical shear rate as the point at which $A_{\mathrm{TAN}} = 0.5$ (although the transition is so abrupt that this choice does not affect the interpretation). Using the measured bending modulus for CPCl-hexanol membranes [35,36] of $\sim 1 k_B T$, the solvent viscosity of 16.3 cP, and a prefactor of 1, the prediction of Bruinsma and Rabin [27] becomes $\dot{\gamma}_c = 2.5 \times 10^8 d^{-3}$, where d (nm) is determined from the zero-shear peak position in the ∇V direction. Figure 4 shows the experimental variation of critical shear rate with interlamellar separation, together with the predictions of Bruinsma and Rabin. The theory makes excellent quantitative predictions for membranes up to $\phi = 0.05$ ($d > 65$ nm), but deviates from experiment at higher concentrations. This is perhaps not surprising, as their calculations assume that neighbors act only to constrain the average amplitude of fluctuations, neglecting coupling and collective motions.

A frequent question in membrane dynamics is whether the solvent viscosity or the sample viscosity is the relevant parameter to use in shear flow treatments. Al kahwaji *et al.* incorporated the lamellar periodicity dependence of the zero-shear viscosity ($\eta \sim 1/d^2$), measured in a Couette cell, for their thin film results in order to match the theoretical predictions for the onset of turbidity defining the threshold shear rate for lamellar collapse. In Fig. 3 we have used solvent viscosity, as we did in our previous studies of sponge phases in this system, on the grounds that collapse is a local phenomenon occurring between membranes, like membrane fusion [6,7,10]. However, it is also clear empirically that to use sample viscosity, which increases with membrane volume fraction, would lead to a much higher-order d dependence and poorer agreement with theoretical scaling behavior.

The effect of shear on smectic lyotropic phases has recently attracted theoretical interest since it triggers such a rich range of experimental behaviors. Shear effects on membrane undulations have been theoretically addressed, but experiments have not yet been able to validate these predictions, as two opposing effects influence the membrane fluctuation spectrum. Amplification of fluctuations (Reynolds effect) comes from coupling between shear flow and membrane elastic stress, which slows fluctuation relaxation and increases their lifetime, leading to stronger smectic order. This effect is visible only in a limited Q range close to the Bragg peak, and we have not attempted to characterize it further because of the low resolution of SANS. When the shear rate approaches or exceeds the characteristic lifetime of the fluctuation, the membrane is so severely stretched by the elastic deformation that the energy cost to sustain the fluctuation dramatically increases, leading to a reduction of the fluctuation

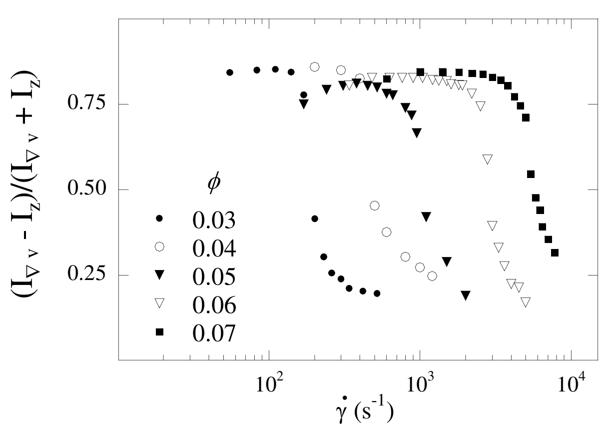

FIG. 3. Tangential geometry scattering anisotropy of the lamellar phase $A_{\mathrm{TAN}} = (I_{\nabla V} - I_Z)/(I_{\nabla V} + I_Z)$ as a function of shear rate, $\dot{\gamma}$, for membrane volume fractions $\phi = 0.03$–0.07.

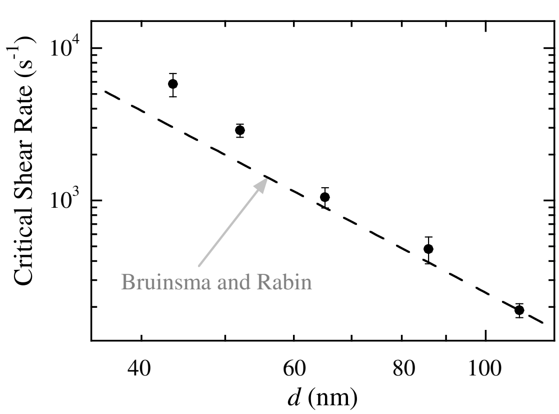

FIG. 4. Variation of the critical shear rate for collapse, $\dot{\gamma}_c$, with interlamellar spacing, d, with predictions of the model of Bruinsma and Rabin [27], showing the d^{-3} dependence. Error bars show shear rates determined for $A_{\mathrm{TAN}} = 0.4$ and 0.6.

lifetime (Maxwell effect). In the present case, the slowest relevant undulations are those of a wavelength equal to the patch size or collision length responsible for steric repulsions. When the imposed flow field ''irons out'' these fluctuations, the lamellar phase loses is stability and the phase collapses. Recent theories have predicted a change in the shape of the lamellar diffraction peak prior to collapse by including an anisotropic membrane tension as the stress component of the flow [24].

Above $\dot{\gamma}_c$, $I_Z(Q)$ and $I_{\nabla V}(Q)$ display an approximately Q^{-2} dependence (not shown) as expected for a bilayer, which may indicate an aligned tubular vesicle structure in the flow direction (see Fig. 1 at 2000 s^{-1}). However, a wider Q range and improved signal-to-noise ratio is needed to fully characterize this state and the structural changes preceding collapse.

We have shown that an equilibrium lamellar phase with a low defect density shear aligned in a c orientation can exhibit a dramatic instability above a critical shear rate, leading to its collapse. This abrupt transition depends sensitively on membrane spacing. Theoretical predictions give good quantitative agreement with measured critical shear rates for dilute samples ($\phi < 0.05$), but the results suggest that some assumptions need to be reexamined or higher-order corrections incorporated in order to understand higher membrane concentration behavior. A number of other lamellar systems will be investigated in order to elucidate the dependence of the critical shear rate on the membrane spacing, bending moduli, and solvent viscosity.

The observation of the collapsed state from a sheared lamellar phase requires a very low concentration of defects such as focal conics in the quiescent solution, which might otherwise trigger another type of instability leading to the formation of onions. To observe collapse, we specifically tuned the structure and dynamics in the lamellar phase. First, the solvent viscosity was increased by dextrose to slow membrane dynamics. Second, the membrane composition was chosen so that the lamellar phase is close to the L_3/L_a biphasic region, where the Gaussian bending modulus $\bar{\kappa}$ is positive and the lamellar phase is sparse in defects (in contrast with $\bar{\kappa} < 0$ where the lamellar phase presents many spherulites). The effect of shear on a lamellar phase in which the composition is varied to control defect density and Gaussian curvature is currently being examined to determine whether onion formation prevents collapse.

The NG7 SANS instrument is operated by the NIST, U.S. Department of Commerce, with funding from the U.S. National Science Foundation under Agreement No. DMR-9986442. Certain commercial materials and equipment are identified in this Letter. In no case does such identification imply recommendation by the National Institute of Standards and Technology. This work was sponsored by the Laboratory Directed Research and Development Program of Oak Ridge National Laboratory, managed by UT-Battelle, LLC for the U.S. Department of Energy under Contract No. DE-AC05-00OR22725. G. G. W. acknowledges support from the University of Sydney Special Studies Program.

[1] D. D. Lasic, *Liposomes: From Physics to Applications* (Elsevier, New York, 1993).
[2] W. Helfrich, J. Phys. Condens. Matter **6**, A79 (1994); G. Porte, J. Phys. Condens. Matter **4**, 8649 (1992), and references therein.
[3] W. M. Gelbart, A. Ben-Shaul, and D. Roux, *Micelles, Membranes, Microemulsion and Monolayers* (Springer, Berlin, 1994).
[4] G. Porte, Curr. Opin. Colloid Interface Sci. **1**, 345 (1996), and references therein.
[5] R. Lipowsky and E. Sackmann, *Structure and Dynamic of Membranes* (Elsevier, Amsterdam, 1995).
[6] L. Porcar *et al.*, Phys. Rev. Lett. **89**, 168301 (2002).
[7] L. Porcar *et al.*, Langmuir **19**, 10 779 (2003).
[8] G. Porte *et al.*, J. Phys. II (France) **1**, 110 (1991).
[9] M. E. Cates and S. T. Milner, Phys. Rev. Lett. **62**, 1856 (1989).
[10] L. Porcar *et al.*, Phys. Rev. Lett. **93**, 198301 (2004).
[11] O. Diat, D. Roux, and F. Nallet, J. Phys. II (France) **3**, 1427 (1993).
[12] J. Zipfel *et al.*, J. Phys. Chem. B **103**, 2841 (1999).
[13] M. Miecowicz, Nature (London) **158**, 27 (1946).
[14] C. R. Safinya *et al.*, Science **261**, 588 (1993).
[15] M. E. Cates and S. T. Milner, Phys. Rev. Lett. **62**, 1856 (1989).
[16] O. Diat and D. Roux, J. Phys. II (France) **3**, 9 (1993).
[17] T. Gulik-Krzywicki *et al.*, Langmuir **12**, 4668 (1996).
[18] D. D. Lasic, *Liposomes* (Elsevier, New York, 1993).
[19] A. Bernheim-Grosswasser *et al.*, J. Chem. Phys. **112**, 3424 (2000).
[20] P. Couvreur *et al.*, *Microencapsulation: Method and Industrial Application*, edited by S. Benita (Marcel Dekker, New York, 1996).
[21] D. Roux and F. Gauffre, Eur. Chem. Chronicle **2**, 17 (1998).
[22] A. G. Zilman and R. Granek, Eur. Phys. J. B **11**, 593 (1999).
[23] A. S. Wunenberger *et al.*, Eur. Phys. J. E **2**, 277 (2000).
[24] S. W. Marlow and P. D. Olmsted, Eur. Phys. J. E **8**, 485 (2002).
[25] J. Zipfel *et al.*, J. Phys. Chem. B **103**, 2841 (1999).
[26] O. Dhez, F. Nallet, and O. Diat, Europhys. Lett. **55**, 821 (2001).
[27] R. Bruinsma and Y. Rabin, Phys. Rev. A **45**, 994 (1992).
[28] S. Ramaswamy, Phys. Rev. Lett. **69**, 112 (1992).
[29] A. Al kahwaji and H. Kellay, Phys. Rev. Lett. **84**, 3073 (2000).
[30] J. Yamamoto and H. Tanaka, Phys. Rev. Lett. **74**, 932 (1995).
[31] V. Chen, Ph.D. thesis, University of Minnesota, 1988.
[32] L. Porcar *et al.*, Rev. Sci. Instrum. **73**, 2345 (2002).
[33] A. Caillé, C. R. Acad. Sci. Paris Ser. B **274**, 891 (1972).
[34] F. Nallet, R. Laversanne, and D. Roux, J. Phys. II (France) **3**, 487 (1993).
[35] D. Roux *et al.*, Europhys. Lett. **17**, 575 (1992).
[36] G. Bouglet and C. Ligoure, Eur. Phys. J. B **9**, 137 (1999); G. Bouglet (private communication).